Strong asymmetry for surface modes in nonlinear lattices with long-range coupling

Alejandro J. Martínez, Rodrigo A. Vicencio, and Mario I. Molina

Departamento de Física, Facultad de Ciencias, Universidad de Chile, Santiago, Chile and Center for Optics and Photonics,
Universidad de Concepción, Casilla 4016, Concepción, Chile

We analyze the formation of localized surface modes on a nonlinear cubic waveguide array in the presence of exponentially decreasing long-range interactions. We find that the long-range coupling induces a strong asymmetry between the focusing and defocusing cases for the topology of the surface modes and also for the minimum power needed to generate them. In particular, for the defocusing case, there is an upper power threshold for exciting staggered modes, which depends strongly on the long-range coupling strength. The power threshold for dynamical excitation of surface modes increases (decreases) with the strength of long-range coupling for the focusing (defocusing) cases. These effects seem to be generic for discrete lattices with long-range interactions.

I. INTRODUCTION

Arrays of coupled optical waveguides and periodic photonic lattices constitute a current area of intense research activity due to the rich physical phenomena that arise when combining discreteness, periodicity, nonlinearity, and surface effects [1]. In addition to the interest stemming from the creation and controlling of the propagation of light beams for their potential use in multiport switching and routing of signals for envisioned all-optical devices, "discrete optics" has also recently become one of the favorite tools for direct observation of phenomena associated with discrete, periodic media, such as Bloch oscillations [2], Anderson localization [3], and discrete breathers and solitons [4], to name a few.

A substantial amount of work has been devoted to the case of weakly coupled nonlinear waveguide arrays, where the mode overlap between neighboring guides is small, and the nonlinearity is strictly local. Recent experimental and theoretical work in realistic systems, such as dipole-dipole interactions in Bose-Einstein condensates (BECs) [5] and discrete light localization in nematic liquid crystals [6], has stimulated research into the effects of nonlocal effects. In general, nonlocal nonlinearity tends to stabilize several types of solitons, such as dark solitons in three-dimensional (3D) dipolar BECs [7], chirp-imprinted spatial solitons in nematic liquid crystals [6], optical vortex solitons [8], rotating dipole solitons [9], and azimuthons [10]. The effect of long-range dispersive interactions, on the other hand, has received comparatively less attention. The effect of power-law dispersion on anharmonic chains [11], as well as the inclusion of second-order coupling in optical waveguide arrays [12,13], suggests the onset of bistable effects. Although at first glance the inclusion of long-range coupling would seem to lead to an increase of the power level needed to excite a localized mode [12], there are also some counterintuitive results for the case of a single nonlinear (cubic) defocusing impurity. There, a small addition of coupling to second nearest neighbors actually *decreases* the power threshold for the generation of a localized mode [14].

On the other hand, surface states have attracted considerable attention of the community during the past five years. Unlike the case of fundamental bulk modes, where there is no minimum power to excite them, for one-dimensional (1D)

surface states there is a power threshold for their excitation. When only nearest-neighbor interactions are considered, this power is independent of the sign of the nonlinearity [15].

In this work we examine the formation and stability of localized surface modes in a nonlinear optical waveguide array with realistic-looking long-range coupling (see Fig. 1). The semicircular geometry is a possible experimental configuration where one could find long-range coupling effects. We find a striking asymmetry between the behavior of the focusing and defocusing cases, as the coupling range is varied. Contrary to what occurs in a focusing case, for a defocusing nonlinearity an increase in coupling range actually reduces the amount of power needed to generate a surface localized stationary mode. This counterintuitive result also holds for the dynamical excitation of the surface mode from a narrow input beam. In addition, we found an *upper threshold* for the excitation of staggered states, effect that could be experimentally observed in current zigzag arrays [13].

This paper is organized as follows. In Sec. II we introduce our model of a nonlinear waveguide array with exponentially decreasing long-range interactions. Section III is devoted to the dispersion relation for the linear plane waves. In Sec. IV we examine the nonlinear surface localized modes of the model, and focus on the asymmetry introduced by the long-range coupling, between the focusing and defocusing cases, as far as topology and minimum power requirements are concerned. In Sec. V we examine the effects of long-range coupling on the dynamical evolution of an initially localized input beam, revealing the diametrically opposite behavior of the self-trapped portion between the focusing and defocusing cases. Finally, Sec. VI concludes the paper.

II. MODEL

Let us consider a finite array of single-mode, nonlinear (Kerr) optical waveguides including higher-order coupling among sites. In the coupled-mode framework, the system is described by a discrete nonlinear Schrödinger (DNLS) equation:

$$i\frac{du_n}{dz} + \sum_{m \neq n} V_{n,m} u_m + \gamma |u_n|^2 u_n = 0, \tag{1}$$
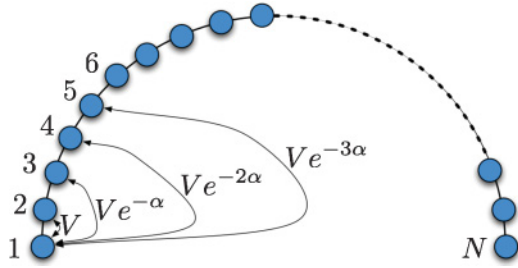
FIG. 1. (Color online) N-site waveguide array with long-range coupling.

where u_n is the amplitude of the waveguide mode in the nth waveguide, z is the propagation distance along the array, γ is the nonlinear parameter, and the coefficient $V_{n,m}$ is the coupling between the nth and mth guides. To be consistent with the coupled-mode approach, we will model $V_{n,m}$ as $V_{n,m} = Ve^{-\alpha(|n-m|-1)}$, where V is the usual coupling coefficient to nearest neighbors and $\alpha > 0$ is the strength for the long-range interaction. A large α value implies interaction with essentially one site (DNLS limit), while a small α increases the coupling range.

The power, defined as $P = \sum_n |u_n|^2$, is a conserved quantity of model (1), and we will use it to characterize nonlinear modes. We look for stationary solutions of the form $u_n(z) = u_n \exp(i\lambda z)$ of model (1), obtaining

$$\lambda u_n = \sum_{m \neq n} Ve^{-\alpha(|n-m|-1)} u_m + \gamma u_n^3 , \qquad (2)$$

where $u_n \in \text{Re}$ and λ is the propagation constant.

III. LINEAR PROPERTIES

To obtain the dispersion relation for linear plane waves, we set $\gamma = 0$ and insert a solution $u_n = U \sin(kn)$ in Eq. (2), obtaining

$$\lambda(k,\alpha) = V \left(\frac{e^\alpha \cos k - 1}{\cosh \alpha - \cos k} \right), \qquad (3)$$

where k is the transversal wave number. Figure 2(a) shows linear band regions for different values of α. The edges of these bands are located at $\lambda_{\min} \equiv \lambda(\pi,\alpha) = -2V/[1 + \exp(-\alpha)]$ and $\lambda_{\max} \equiv \lambda(0,\alpha) = 2V/[1 - \exp(-\alpha)]$, where the limit $N \to \infty$ has been assumed. The width $\lambda_{\max} - \lambda_{\min} = 4V/[1 - \exp(-2\alpha)]$ increases as soon as coupling beyond nearest neighbors is considered. As a consequence, the existence region for staggered solutions [$\lambda \in \{-\infty, \lambda_{\min}\}$] increases with α while the corresponding region for unstaggered solutions [$\lambda \in \{\lambda_{\max}, \infty\}$] decreases. Figures 2(b) and 2(c) show profiles for $\lambda_{\min}$ and $\lambda_{\max}$ with staggered [$(-1)^n u_n$] and unstaggered ($u_n > 0 \, \forall \, n$) topologies, respectively.

IV. NONLINEAR SURFACE MODES

Next, we compute nonlinear stationary surface solutions for focusing ($\gamma > 0$) and defocusing ($\gamma < 0$) nonlinearities by implementing a multidimensional Newton-Raphson method [15]. A linear stability analysis reveals that the Vakhitov-Kolokolov criterion still holds in the presence of long-range coupling, i.e., $\partial P/\partial \lambda > 0$ implies stability. The P vs λ curves
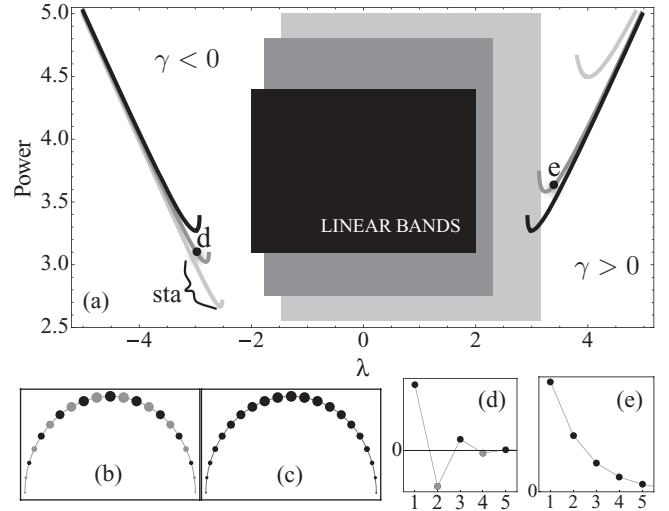
FIG. 2. (a) P vs λ diagrams (including linear bands) for $\alpha = 6$ (black), 2 (gray), and 1 (light gray), for focusing and defocusing cases. (b) and (c) Linear modes for $k = \pi$ and $k = 0$, respectively. (d) and (e) Nonlinear surface modes for points marked in (a). $V = |\gamma| = 1$ and $N = 100$. Black (gray) points in profiles denote $u_n > 0$ (<0). The sizes of the dots in (b) and (c) are proportional to the amplitudes, while the black (gray) colors in (b) and (d) denote positive (negative) amplitudes.

for these modes show an important asymmetry between the focusing and defocusing cases [see Fig. 2(a)]: In the short-range coupling case ($\alpha = 6$, black curves), power thresholds (P_{th}) for positive and negative γ are equal, as in a DNLS lattice [15]. However, when long-range coupling is relevant ($\alpha \ll 6$), P_{th} increases as α decreases in the focusing case. On the contrary, for $\gamma < 0$ this threshold decreases when α decreases [see gray and light-gray curves in Fig. 2(a)].

An explanation for the P_{th} asymmetry can be the following: We start from a surface profile, such as the ones shown in Figs. 2(d) and 2(e), with the general form $u_0\{1,\epsilon,\beta,\xi,\ldots\}$ with $1 > |\epsilon| > |\beta| > |\xi| > \cdots$. By inserting this ansatz in Eq. (2) for $n = 1$, we get $\lambda = V(\epsilon + \beta e^{-\alpha} + \xi e^{-2\alpha} + \cdots) + \gamma u_0^2$. Since discrete solitons exist outside of linear bands, fundamental localized solutions would, in principle, bifurcate exactly at the frontiers of these bands, depending on the sign of nonlinearity. Let us discuss first the *unstaggered case* and try to get an estimate for P_{th} in terms of α. It is well known that when the solution approaches the linear band ($\lambda \to \lambda_{\max}$), its power decreases and it becomes more and more extended (delocalized) [1,4]. This implies that (in such a limit) $\epsilon,\beta,\xi,\ldots \to 1$ (this limit is exactly the opposite of the one occurring for a high level of power, where solutions are extremely localized and $\epsilon,\beta,\xi,\ldots \to 0$). Therefore, $1 + e^{-\alpha} + e^{-2\alpha} + e^{-3\alpha} + \cdots = 1/(1 - e^{-\alpha})$, implying that $\lambda \to V/(1 - e^{-\alpha}) + \gamma u_0^2$. However, this would imply that, for $u_0 \to 0$, $\lambda < \lambda_{\max}$, which is certainly a contradiction because the fundamental unstaggered solution could originate from the top of the band but not inside of the band. As a consequence, at least $\gamma u_0^2 \approx V/(1 - e^{-\alpha})$. Since power is directly proportional to u_0^2, we obtain the estimate $P_{\text{th}} \sim 1/(1 - e^{-\alpha})$. Thus, for $\gamma > 0$, P_{th} will be a decreasing function of α, diverging at $\alpha = 0$, and remaining finite at $\alpha \gg 0$. On the other hand, for
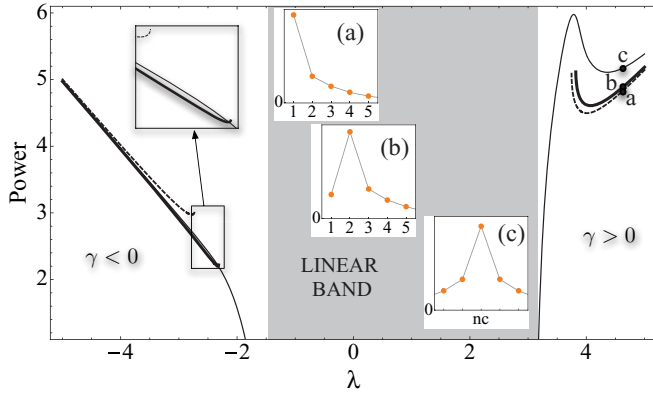
FIG. 3. (Color online) P vs λ diagrams for modes centered at $n = 1$ [(a) dashed line], $n = 2$ [(b) thick line], and $n = n_c$ [(c) thin line]. $V = |\gamma| = \alpha = 1$ and $N = 2n_c = 100$.

FIG. 4. Existence regions in α-λ space. The light-gray area corresponds to unstaggered ($\lambda > 0$) and staggered ($\lambda < 0$) solutions. The gray area represents the linear band while the white area denotes no solutions. The black region denotes solutions with no well-defined topology. Insets show examples of mode profiles in several regions.

$\gamma < 0$, the situation is quite different. First, there is no trivial transformation between unstaggered and staggered solutions as in the nearest-neighbor DNLS model. However, again, while the localized solution approaches the linear band ($\lambda \rightarrow \lambda_{\min}$), its power decreases and it becomes more delocalized, but now the solution is staggered. That implies a sign difference between nearest-neighbor amplitudes in the same way as for the fundamental linear mode located at $\lambda_{\min}$ [see Fig. 2(b)]. Therefore, $\epsilon, -\beta, \xi, \ldots \rightarrow -1$. Now we solve the sum $1 - e^{-\alpha} + e^{-2\alpha} - e^{-3\alpha} + \cdots = 1/(1 + e^{-\alpha})$, implying that $\lambda \rightarrow -V/(1 + e^{-\alpha}) - |\gamma|u_0^2$. For $u_0 \rightarrow 0$, $\lambda > \lambda_{\min}$, i.e., a contradiction. Again, at least $|\gamma|u_0^2 \approx V/(1 + e^{-\alpha})$, so $P_{\text{th}} \sim 1/(1 + e^{-\alpha})$. Thus, for $\gamma < 0$, P_{th} is an increasing function of α with a minimum at $\alpha = 0$. Our analytical estimates agree perfectly with the numerical behavior presented in Fig. 2(a).

We also computed localized solutions centered below the surface in order to detect the onset of the bulk phenomenology (see Fig. 3). For $\gamma > 0$, the power as a function of λ shows the onset of a bistable curve for $\alpha \lesssim 1.69$. This feature was observed before in the context of a zigzag model [12,13], and seems to reflect an increase in effective dimensionality as soon as coupling beyond nearest neighbors becomes important. The most salient feature is that, in this case, the threshold power to create a mode behaves in a manner opposite to that of the usual DNLS. For example, for $\alpha = 1$, Fig. 3 shows that, for $\gamma > 0$, the minimum required power (P_{th}) for creating an unstaggered localized solution increases as the mode center is located further away from the surface. In that sense, *the system favors the localization of energy at the boundary for $\gamma > 0$*, contrary to the usual 1D DNLS model [15] (around $\alpha \approx 1.3$, the DNLS phenomenology transforms into the long-range one). On the other hand, the system asymmetry is manifest for $\gamma < 0$; the P_{th} for exciting a staggered localized mode decreases as the mode center is pushed away from the surface. Now, the system does not favor the generation of discrete surface solitons, as in the usual DNLS.

Fundamental nonlinear modes are unstaggered for $\gamma > 0$ and staggered for $\gamma < 0$. As the power content of the mode is increased, we find that unstaggered modes retain their character, as expected for high-power solutions. However, contrary to what is expected, for staggered modes, a new power threshold P_{up} appears where the staggered topology

of the mode is lost. Figure 4 shows the existence regions for unstaggered and staggered solutions in α-λ space. We see that unstaggered solutions exist from some minimum λ value (surface threshold) up to infinite. On the contrary, for $\gamma < 0$ the staggered mode is well defined from the surface threshold value (which depends weakly on α) up to a second λ value (with power P_{up}) that increases monotonically with α. Close to, but beyond this second threshold, the mode is no longer staggered because, although it retains some oscillations of the mode phases, it does not preserve a full staggered topology. As λ decreases, the alternating phase topology is lost altogether. The white thick line separating the light-gray and black regions is a result of asking the solution if $u_3 < 0$, as an indicator of the change of topology in the central region. Figure 4(a) shows a mode example where all lattice sites are negative except for the first one, i.e., the mode is by definition not staggered. In the numerical continuation there is no evidence of this change on topology [see "sta" in Fig. 2(a) for $\gamma < 0$ and $\alpha = 1$]. Curves are monotonic and the only way to observe this phenomenology is by taking a close look at the phase structure.

We can use a strongly localized mode approximation to give an explanation for this unexpected behavior occurring for $\gamma < 0$. This approach is valid when the propagation constant is far from the linear band, where the mode can be approximated as $\{u_n\} = u_0\{1, \epsilon, \beta, 0, \ldots\}$, and $1 \gg |\epsilon| \gg |\beta|$. We concentrate the analysis in the parameter β as an indicator of the long-range interaction effect. If we insert this ansatz in Eq. (2) and solve it for site $n = 3$, we obtain $\beta \approx V(\epsilon + e^{-\alpha})/(\lambda - \gamma u_0^2\beta^2)$. From the anticontinuous limit, we know that high-power solutions consist essentially of one excited amplitude plus some exponentially small tails. Therefore, as a first approximation, $|\lambda| \gtrsim |\gamma|u_0^2$. If $\gamma > 0$, also $\lambda, \epsilon > 0$ [see Figs. 2(a) and 2(e)], implying that $\beta > 0$ for any α. This shows us that, for a focusing case, solutions preserve their phase in the whole range of parameters. On the contrary, when $\gamma < 0$, also $\lambda, \epsilon < 0$ [see Figs. 2(a) and 2(d)]; therefore, the sign of β will depend on the balance $|\epsilon| - e^{-\alpha}$. For a
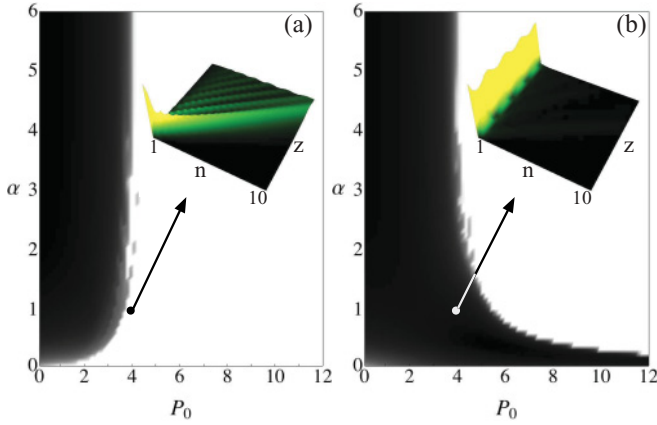
FIG. 5. (Color online) Output power fraction in P_0-α space. (a) and (b) correspond to $\gamma < 0$ and $\gamma > 0$, respectively. Dark and light regions denote $f = 0$ and $f = 1$, respectively. Insets: Dynamical propagation for $\alpha = 1$ and $P_0 = 4$.

fixed α, this balance will be negative always for high-power solutions because $\epsilon \to 0$ (anticontinuous limit). Therefore, for a large α, an upper power threshold is expected to appear at high frequencies; for smaller α, this threshold is expected to occur closer to the band because ϵ is also larger there. This agrees perfectly with the thick white line of Fig. 4.

V. DYNAMICS

We also looked into the effects of long-range coupling on the dynamical evolution of an initially localized input beam. We solved Eq. (1) numerically with an initial condition of $u_n(0) = \sqrt{P_0}\delta_{n,1}$, where P_0 is the input power. For a given α and P_0, we computed the space-averaged fraction of power remaining at the initial waveguide f, after a longitudinal

propagation distance: $f = (P_0 z_{\max})^{-1} \int_0^{z_{\max}} |u_1(z)|^2 dz$. Results for f as a function of α and P_0 are shown in Fig. 5 in the form of a density plot. Its most striking feature is the diametrically opposite self-trapping behavior between $\gamma > 0$ and $\gamma < 0$. While in the first case [Fig. 5(b)] an increase in coupling range (decreased α) increases the threshold power for self-trapping, in the second case, a greater coupling range implies a smaller power threshold. This counterintuitive asymmetry becomes particularly strong around $\alpha \sim 1$ (see insets). These results are in complete agreement with the ones obtained for the stationary modes.

Finally, we repeated all of the above studies on a simpler but related model that is amenable to direct experimental probing—the zigzag model [12]—and have verified the strong asymmetry effects for the formation of localized surface modes at both the stationary and dynamics level. This opens the door to a direct experimental verification of these effects.

VI. CONCLUSIONS

In conclusion, we have examined the formation of localized surface modes on a nonlinear waveguide array in the presence of realistic long-range interactions, and found a strong asymmetry between the focusing and defocusing cases for the mode topology and the minimum power to effect a localized surface mode. We believe these effects are generic to discrete nonlinear systems with long-range coupling.

ACKNOWLEDGMENTS

[1] F. Lederer, G. I. Stegeman, D. N. Christodoulides, G. Assanto, M. Segev, and Y. Silberberg, Phys. Rep. **463**, 1 (2008).

[2] R. Morandotti, U. Peschel, J. S. Aitchison, H. S. Eisenberg, and Y. Silverberg, Phys. Rev. Lett. **83**, 4756 (1999).

[3] T. Schwartz, G. Bartal, S. Fishman, and M. Segev, Nature (London) **446**, 52 (2007).

[4] S. Flach and A. Gorbach, Phys. Rep. **467**, 1 (2008).

[5] M. Klawunn and L. Santos, Phys. Rev. A **80**, 013611 (2009).

[6] A. Fratalocchi and G. Assanto, Phys. Rev. E **72**, 066608 (2005).

[7] R. Nath, P. Pedri, and L. Santos, Phys. Rev. Lett. **101**, 210402 (2008).

[8] A. A. Minzoni, N. F. Smyth, Z. Xu, and Y. S. Kivshar, Phys. Rev. A **79**, 063808 (2009).

[9] S. Lopez-Aguayo, A. S. Desyatnikov, Y. S. Kivshar, S. Skupin, W. Krolikowski, and O. Bang, Opt. Lett. **31**, 1100 (2006).

[10] S. Lopez-Aguayo, A. S. Desyatnikov, and Y. S. Kivshar, Opt. Express **14**, 7903 (2006).

[11] Yu. B. Gaididei, S. F. Mingaleev, P. L. Christiansen, and K. Ø. Rasmussen, Phys. Lett. A **222**, 152 (1996); K. Ø. Rasmussen, P. L. Christiansen, M. Johansson, Yu. B. Gaididei, and S. F. Mingaleev, Physica D **113**, 134 (1998); S. F. Mingaleev, Yu. B. Gaididei, and F. G. Mertens, Phys. Rev. E **58**, 3833 (1998); S. Flach, *ibid.* **58**, R4116 (1998).

[12] N. K. Efremidis and D. N. Christodoulides, Phys. Rev. E **65**, 056607 (2002).

[13] A. Szameit, T. Pertsch, S. Nolte, A. Tünnermann, and F. Lederer, Phys. Rev. A **77**, 043804 (2008); A. Szameit, R. Keil, F. Dreisow, M. Heinrich, T. Pertsch, S. Nolte, and A. Tünnermann, Opt. Lett. **34**, 2838 (2009).

[14] M. I. Molina, Phys. Rev. B **67**, 054202 (2003).

[15] M. I. Molina, R. A. Vicencio, and Yu. S. Kivshar, Opt. Lett. **31**, 1693 (2006); C. R. Rosberg, D. N. Neshev, W. Krolikowski, A. Mitchell, R. A. Vicencio, M. I. Molina, and Yu. S. Kivshar, Phys. Rev. Lett. **97**, 083901 (2006).